A Novel Electrochemical Sensor Based on Flower Shaped Zinc Oxide Nanoparticles for the Efficient Detection of Dopamine

Deepak Balram[1], Kuang-Yow Lian[1,*], Neethu Sebastian[2]

[1] Department of Electrical Engineering, National Taipei University of Technology, No. 1, Section 3, Chung-Hsiao East Road, Taipei 106, Taiwan, Republic of China.
[2] Department of Organic and Polymeric Materials, National Taipei University of Technology, No. 1, Section 3, Chung-Hsiao East Road, Taipei 106, Taiwan, Republic of China.
[*]E-mail: kylian@ntut.edu.tw

In this paper, a novel electrochemical sensor based on flower shaped Zinc Oxide (ZnO) nanoparticles for the determination of dopamine is reported. Flower shaped ZnO nanoparticles is synthesized by a new aqueous solution method without the use of any shape directing reagents and the verification of its successful formation is carried out by scanning electron microscope (SEM) and X-ray diffraction analysis (XRD). Cyclic Voltammetry (CV), Differential Pulse voltammetry (DPV) and amperometric (*i-t*) techniques are used to study the electrochemical characteristics of flower shaped ZnO nanoparticles. In this study, the lower oxidation potential and higher oxidation peak current of flower shaped ZnO modified glassy carbon electrode (GCE) indicates that its electrocatalytic activity is better than bare GCE in the oxidation of dopamine. Even in the presence of common interfacing compounds, the modified GCE exhibited excellent selectivity which is a trait of good electrochemical sensor. The linear response range of the fabricated electrochemical sensor based on flower shaped ZnO nanoparticles is 0.1 - 16 μM, limit of detection is 0.04 μM and the sensitivity is 4.38 $\mu A \mu M^{-1} cm^{-2}$. The low detection limit, excellent sensitivity and wide linear response range signified the efficiency of flower shaped ZnO nanoparticles based electrochemical sensor for the detection of dopamine.

Keywords: Electrochemical sensor, Zinc Oxide nanoparticles, dopamine, detection

1. INTRODUCTION

Nanoparticles possess distinctive physical and chemical properties and this makes them exceptionally fit in the development of advanced electrochemical sensors [1-5]. The small size of nanoparticles adds unique properties and this helps in the development of novel and improved sensors.

Different grades of nanoparticles including metal, oxide, semiconductors and composites are used in the development of electrochemical sensors. In general, the metal nanoparticles exhibit good conductivity and catalytic properties. For electrochemical analysis, semiconductor nanoparticles are usually used as tracers and for the immobilization of biomolecules, oxide nanoparticles are used. For the detection of chemical species based on metal oxide sensors including both transition metal oxides and non-transition metal oxides, several methods are reported [6-9]. ZnO based sensor, which belongs to the category of metal oxide sensor has attained major attention due to the unique properties of ZnO. ZnO is a material having a lot of applications in biosensors, chemical sensors, UV-lasers, piezoelectric devices, gas sensors, UV-photodetectors, transparent electronics, dye-sensitized solar cells and smart windows [10-14]. For the detection of various pollutant gases, ZnO is used as a chemo-resistive sensor. Further, due to the unique properties of ZnO, it is used in a variety of applications including drug delivery, skin lotions, cancer treatment, medical products, sun-screens, bio-imaging etc. [15-18]. The stability of ZnO even at high isoelectric point, small size and powerful binding properties makes it an apt material in the development of electrochemical sensors. The large surface to volume ratio of ZnO nanoparticles is another advantage of using it as a promising material for electrochemical sensing. Different ZnO sensors with various morphological structures such as nanowires [19], nanorods [20], nanopillar [21] and nanorod-bundles [22] has been already reported. The preparation of these nanostructures are based on different techniques such as successive chemical solution deposition [23], thermal evaporation [24], magnetron sputtering [25] etc.

Dopamine is a catecholamine neurotransmitter which plays a major part in the functionality of cardiovascular system and central nervous system [26-29]. DOPA undergoes decarboxylation to form dopamine, which is a precursor of neurotransmitters - noradrenaline and adrenaline. Dopamine affects both behavioral and cognitive functions of living beings and it has a crucial role in memory, learning and attention span [30-33]. In clinical analysis, the presence of dopamine in human body is regularly monitored as it signals drug addiction and Parkinson's disease [34]. Various neurological diseases like schizophrenia, ADHD/ADD, senile dementia and Parkinson's disease are caused because of the complete depletion or low level of dopamine in central nervous system [35-38]. In this regard, the precise and swift determination of dopamine is pivotal and numerous analytical methods with good selectivity and high sensitivity for the determination of dopamine is investigated by researchers. For the effective detection of dopamine, electrochemical sensors are more apt as dopamine is an electrochemically active compound and electrochemical methods are regarded as simple and highly sensitive. In this context, the main aim of this work is the effective detection of dopamine based on electrochemical method.

In this paper, an electrochemical sensor based on flower shaped Zinc Oxide electrode is fabricated for the determination of dopamine. The electrodeposition of Zinc Oxide nanoparticles on the glassy carbon electrode surface is undertaken at ambient conditions. This electrochemical sensor prepared shows high electrocatalytic activity towards dopamine because of the high surface area and good conductivity of ZnO nanoparticles.

2. EXPERIMENTAL SECTION

2.1 Materials and methods

All the chemicals used in the experiment including Zinc Nitrate Hexahydrate $(Zn(NO_3)_2.6H_2O)$, sodium hydroxide (NaOH) and dopamine $(C_8H_{11}NO_2)$ are purchased from Sigma–Aldrich. These chemicals are used without any purification and is of analytical grade. Sodium dihydrogen phosphate (NaH_2PO_4) is mixed with disodium hydrogen phosphate (Na_2HPO_4) for the preparation of 0.05 M phosphate buffer solution (PBS) and we used DI water for preparing all the required solutions.

The morphology and structure of ZnO nanopartricles is characterized by field emission scanning electron microscope. We have used the Hitachi S-4800 scanning electron microscope at 15 KV for this analysis. Bruker D8 Advance X-ray diffractometer (XRD) having monochromatic Cu-Kα radiation ($λ$=1.5418 Å) is used to carry-out the XRD analysis. For performing the electrocatalytic analysis, we used a three-electrode system. In this system, the reference electrode we used is Ag/AgCl-3M KCl, auxiliary electrode is platinum wire and working electrode is the GCE (0.07 cm^2). For amperometric studies, we have used rotating disc glassy carbon electrode (RDGCE) (0.2 cm^2) as the working electrode. The electrochemical techniques including cyclic voltammetry, differential pulse voltammetry and amperometry (i-t) are performed using CHI 405a and CHI 1205a workstation (CH Instruments, USA) for the detection of dopamine.

2.2 Synthesis of flower shaped ZnO

Flower shaped ZnO nanoaggregates were synthesized by aqueous solution method without using any shape directing reagents. In a typical synthesis method, 100 mL of 0.05M $Zn(NO_3)_2.6H_2O$ and 20 mL of 1M NaOH were dissolved in deionized water. The two solutions are preheated at 80°C for 15 minutes. After preheating, the solutions are thoroughly mixed and kept in water bath for 4 hours at 80°C. The resulting white product is centrifuged, washed and dried in oven at 80°C for 12 hours.

2.3 Fabrication of flower shaped ZnO on modified GCE

The flower shaped ZnO nanoparticles is prepared based on aqueous solution method as the initial step of the experiment. Then using 0.05 μM alumina slurry, the GCE is polished well. To eliminate the unwanted alumina particles on the surface of GCE, it is washed using DI water several times. Then, the required weight of ZnO nanoparticles (5 mg/mL) is taken and re-dispersed using de-ionized water. After drop coating the re-dispersed ZnO (optimized concentration; 8 μL) on the GCE, it is dried at room temperature. The unbounded molecules on the surface of GCE is removed by washing the flower shaped ZnO modified GCE using DI water. After the successful fabrication of flower shaped ZnO on GCE, it is further used for the electrochemical analysis.

3. RESULTS AND DISCUSSION

3.1 Characterization of the flower shaped ZnO

The crystal structure of flower shaped ZnO nanoaggregates is examined by X-ray diffraction (XRD) analysis and the resultant pattern is displayed in Fig. 1. All the diffraction peaks are well matched with the wurtzite hexagonal structure of pure ZnO and the diffraction planes corresponding to the flower shaped ZnO are (1 0 0), (0 0 2), (1 0 1), (1 0 2), (1 1 0), and (1 0 3) for the diffraction peaks 31.5, 35.1, 36.9, 48.1, 56.8 and 62.5 respectively (JCPDS Card No. 36-1451) [39]. No extra peaks were observed in the XRD pattern which indicates the formation of pure ZnO and no impurities are present in the synthesized flower shaped ZnO nanoaggregates. The sharp XRD peak reveals the higher crystalline nature of ZnO.
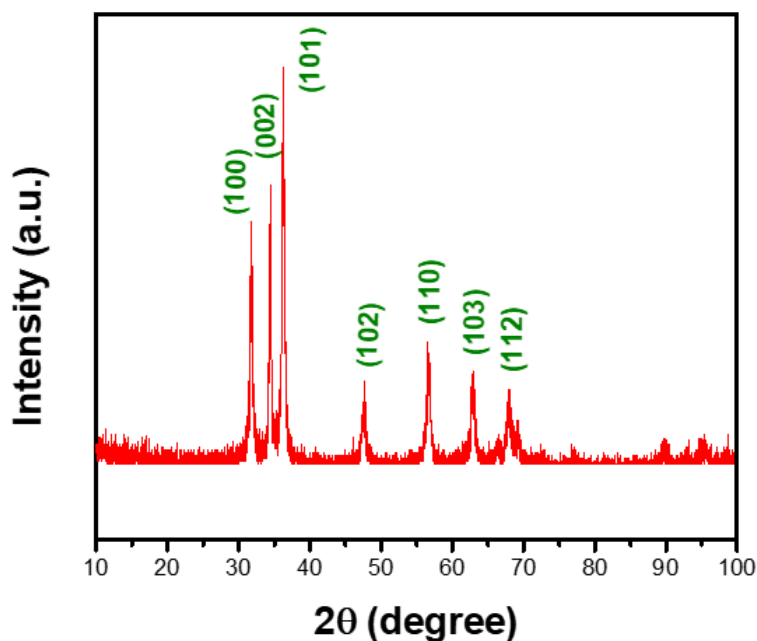

Figure 1. The XRD pattern of as-prepared flower shaped ZnO nanoparticles.

Using the Scherrer's equation, we have calculated the average crystalline size of flower shaped ZnO nanoparticles. Equation 1 given below depicts the Scherrer's equation [40].

$$X_s = \frac{k\lambda}{\beta \cos\theta} \qquad (1)$$

where Xs denotes the crystalline size, k is the Scherrer's constant equal to 0.90, β denotes the full Width at half maximum of high intense diffraction peak, diffraction angle is denoted by θ and the wavelength of X-ray is denoted by λ. The crystalline size of flower shaped ZnO nanoparticles estimated is 21.3 nm, which is the size of a coherently diffracting domain and not compulsorily equal to particle size. The morphological analysis of flower shaped ZnO nanoaggregate is carried out using scanning electron microscopy and the resultant images are given in Fig. 2. The SEM images show a

five to six petal flower shaped morphology for the synthesized ZnO nanoaggregates with the core of each flower having cupola shaped rough surface. The particle size of flower shaped ZnO nanoaggregates is in the range of 400-600 nm.
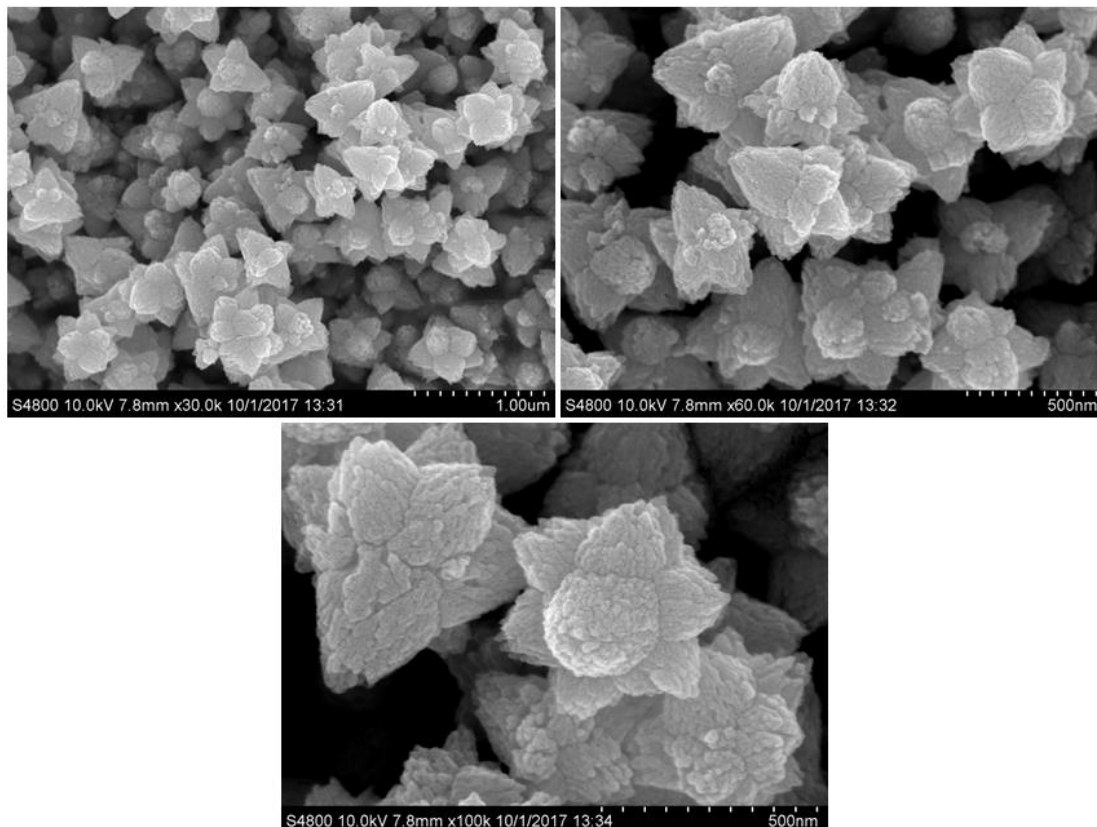

Figure 2. SEM images of flower shaped ZnO nanoparticles with different magnifications.

3.2. Electrochemical behavior of dopamine at flower shaped ZnO modified GCE

Keeping the scan rate constant at 50 mVs^{-1} and considering 0.05 M PBS with same pH value (pH 7.0), the analysis of cyclic voltammograms (CVs) of different electrodes for electrochemical oxidation is carried out and depicted in Fig. 3A. Fig. 3A (a) shows the curve of flower shaped ZnO modified GCE in 0.05 M PBS (pH 7.0) in the presence of 100 μM dopamine at a scan rate of 50 mVs^{1}. In Fig. 3A (b), we have considered flower shaped ZnO modified GCE in the absence of dopamine and Fig. 3A (c) is plotted by considering unmodified GCE in the presence of 100 μM dopamine.
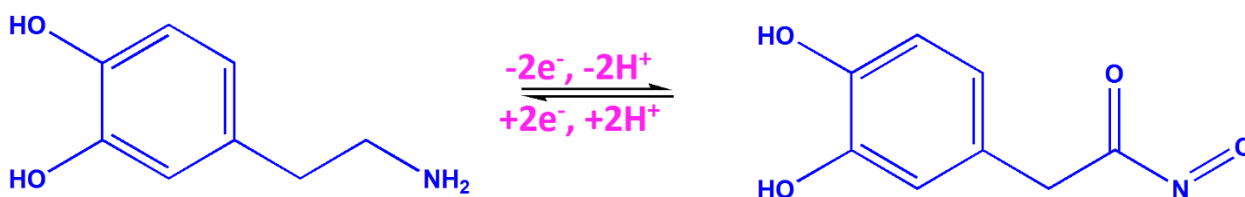
**Scheme 1.** The overall electrochemical mechanism of dopamine.
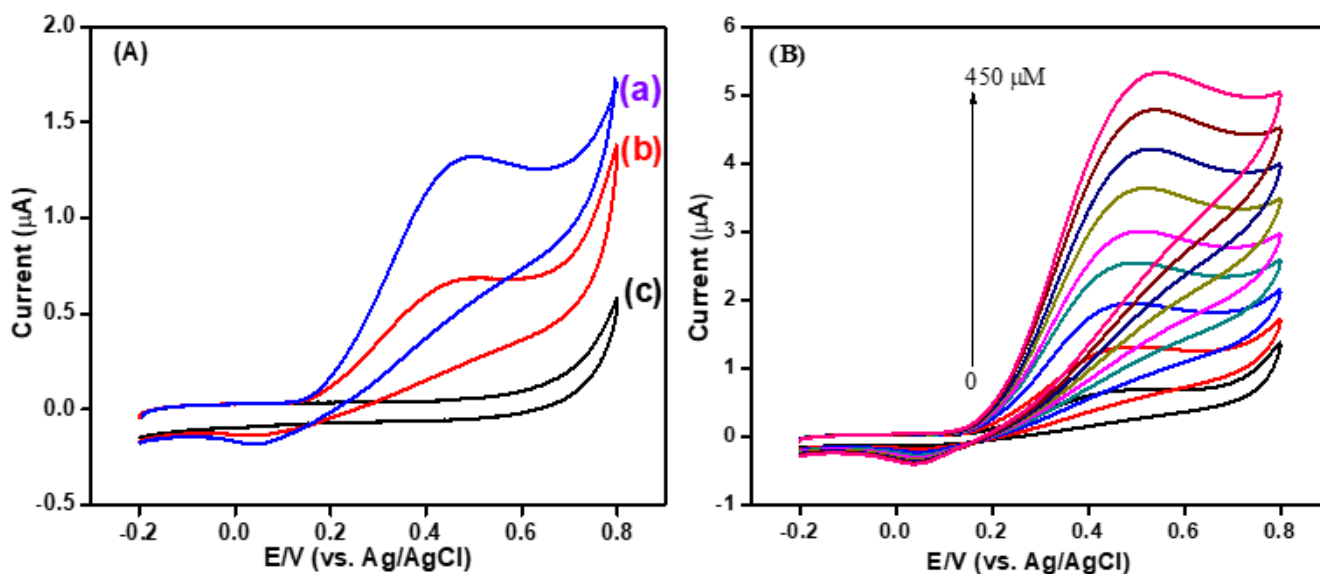
Figure 3. CV curves of modified GCE in the presence (a) and absence (c) of 100 µM dopamine in 0.05M PBS (pH 7.0) at a scan rate of 50 mVs^{-1}, (b) bare GCE in the presence of 100 µM dopamine (A). CV curves of modified GCE in the presence of different concentrations of dopamine (B).

When we compare the three curves, we can see that Fig. 3A (a) has an enhanced anodic peak current and lower positive potential. The oxidation of dopamine to dopamine quinone and reduction of dopamine quinone to dopamine results in a quasi-reversible redox couple which is well-defined [41] as shown in Fig. 3A (a) with an oxidation peak potential of 0.42 V and reduction peak potential of 0.05 V respectively. We haven't observed any redox peak at flower shaped ZnO modified GCE in the absence of dopamine as shown in Fig. 3A (c). This observation signifies that in the potential window range of -0.2 to + 0.8 V, the flower shaped ZnO modified GCE is electrochemically inactive. In Fig. 3A (b), we can observe a lower anodic peak current for unmodified GCE when compared with flower shaped ZnO modified GCE in the presence of dopamine. The reason behind lower anodic peak current of unmodified GCE is the slow electron transfer between electrolyte and electrode surface. Furthermore, when compared with unmodified GCE, it is observed that the anodic peak current at flower shaped ZnO modified GCE in the presence of dopamine is 2.3 fold higher. From the analysis of all the above results, it is clear that flower shaped ZnO modified GCE is a perfect electron mediator for the electrochemical oxidation process of dopamine.

As the next step, we analyze the electrocatalytic activity of flower shaped ZnO modified GCE for the determination of dopamine by following a different approach. For this, by keeping the scan rate constant at 50 mVs^{-1}, we add different amounts of dopamine in 0.05 M PBS (pH 7.0). The resultant plots obtained is depicted in Fig. 3B. Analyzing the curves of different concentration of dopamine as given in Fig. 3B, we can visualize a linear increase in the cathodic and anodic peak current of dopamine as the dopamine concentration increases from 50 to 450 µM. This linear increase is a proof for the excellent electrocatalytic activity of the flower shaped ZnO modified GCE for the detection of dopamine. The unique properties of ZnO including the large surface to volume ratio, powerful binding

properties, small size and good conductivity is the reason for this excellent electrocatalytic activity of flower shaped ZnO modified GCE for the determination of dopamine [42, 43].
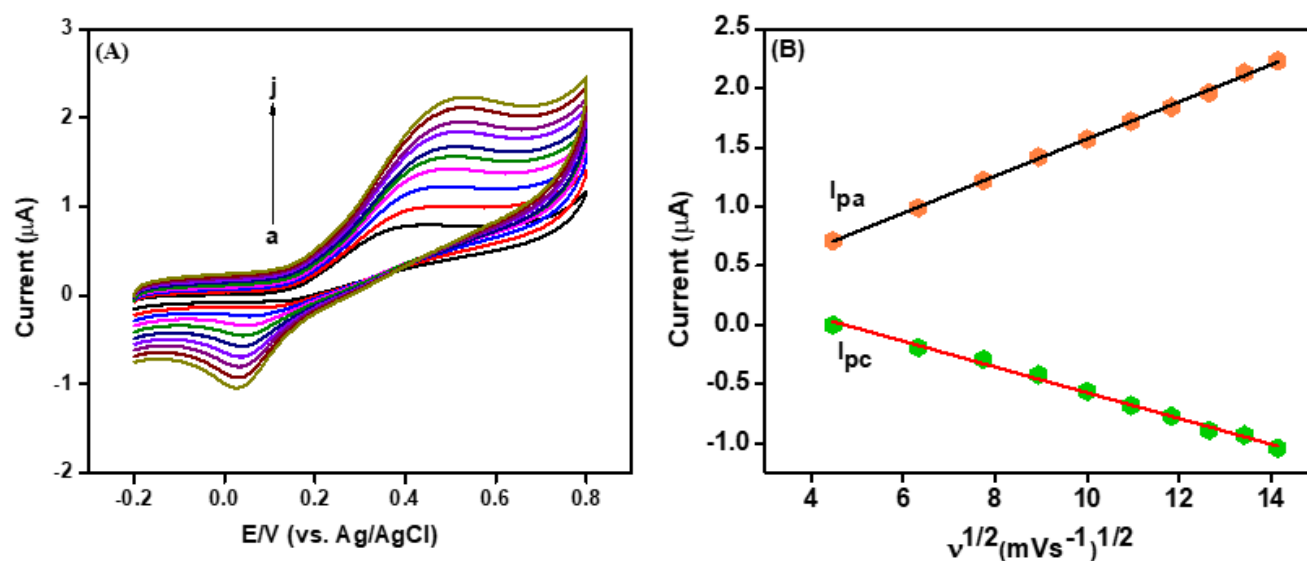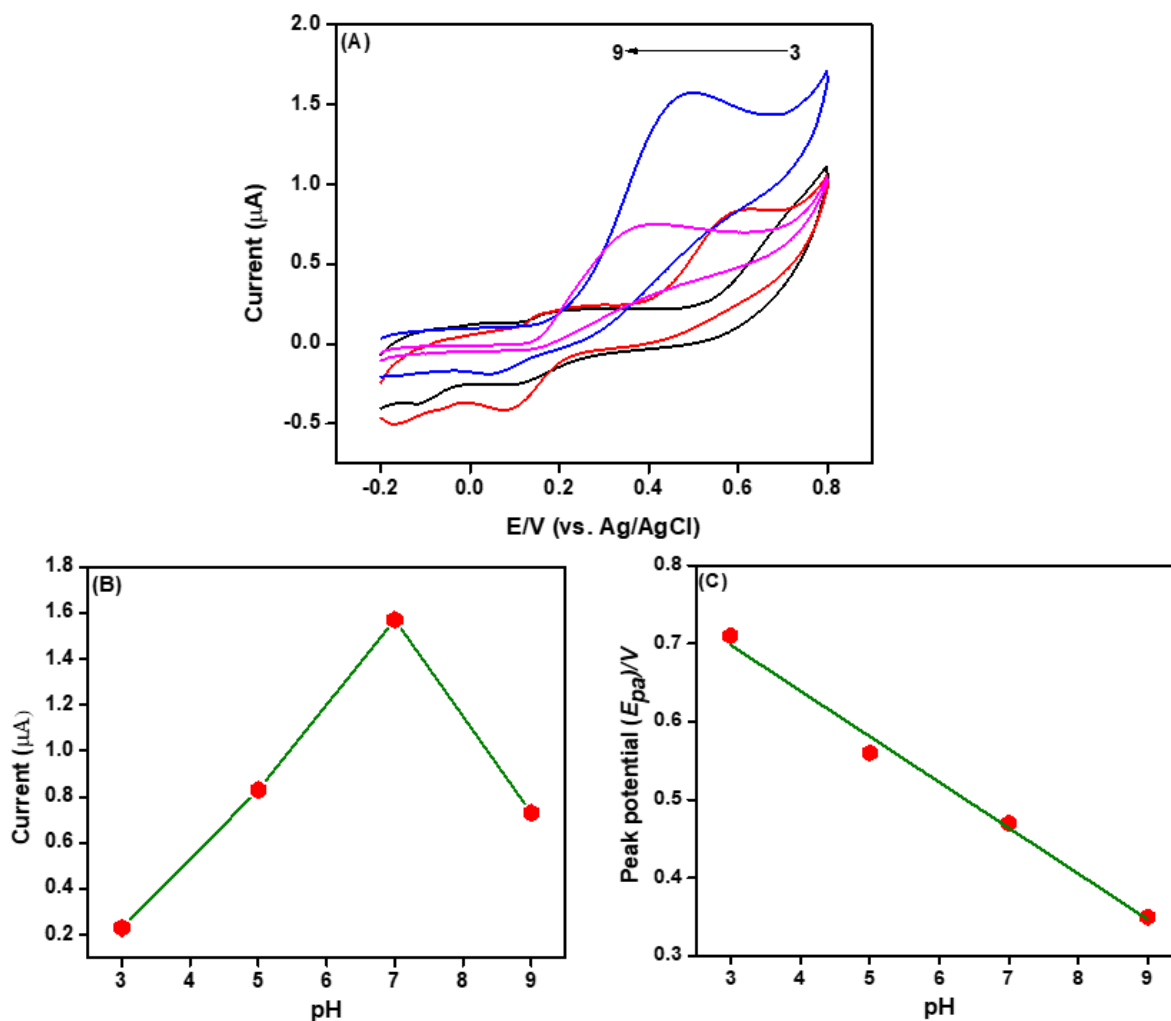

Figure 4. CV curves of flower shaped ZnO modified GCE in the presence of 100 µM dopamine under various scan rates (A). The linear relationship between anodic and cathodic peak current *vs.* scan rate (B).

3.3 The effect of pH and scan rate

The influence of pH and scan rate on the electrocatalytic activity of flower shaped ZnO modified GCE is analyzed as part of the work. The analysis is carried out by keeping the concentration of dopamine constant at 100 µM. The corresponding curves obtained for flower shaped ZnO modified GCE in 0.05 M PBS (pH 7.0) under different scan rates is given in Fig. 4A. The range of scan rate chosen is 20 - 200 mVs^{-1} (20-200; a-j). From Fig. 4A, we can see that an increase of scan rate from 20 - 200 mVs^{-1} results in an increase of both anodic and cathodic peak current of dopamine. So the scan rate is directly proportional to anodic and cathodic peak current of dopamine. Fig. 4B shows the linear plot of anodic and cathodic peak current of dopamine against scan rate. From the linear plot, the linear regression equations can be described as $I_{pa} = 0.1566 + 0.0058$ (µA, mV/s, R^2=0.9991); $I_{pc} = -0.1088 + 0.5161$ (µA, mV/s, R^2=0.9949). From the above results, we can conclude that for different scan rates considered, the electrochemical oxidation of dopamine at flower shaped ZnO is a diffusion controlled electron transfer process rather than adsorption controlled electron transfer process [44].

The effect of pH on electrochemical activity of flower shaped ZnO modified GCE for the detection of dopamine is analyzed in detail. This analysis is vital as pH has significant influence on the oxidation peak potential, peak shape and electrochemical response. The influence of pH on flower shaped ZnO modified GCE for the determination of dopamine is investigated by carrying out studies on different pH values including pH 3.0, pH 5.0, pH 7.0 and pH 9.0 by keeping the amount of

dopamine constant at 100 μM and scan rate 50 mVs^{-1}. The CV response obtained for different pH values is shown in Fig. 5 (A-C).

Figure 5. CV curves of flower shaped ZnO modified GCE in different pH solutions in the presence of 100 μM dopamine at a scan rate of 50 mVs^{-1} (A). Plot of anodic peak current *vs.* pH value (B). Plot of peak potential *vs.* pH value (C).

When we analyze the curves given in Fig. 5, we can see that there is a decrease in the oxidation peak current as the pH value increases from 7.0 to 9.0 and there is an increase in the oxidation peak current from 3.0 to 7.0. From this analysis, it is clear that the oxidation peak current of dopamine is maximum at pH 7.0. Therefore, for the electrochemical detection of dopamine based on flower shaped ZnO modified GCE, we have taken pH 7.0 as the best electrolyte. The linear plot of pH value vs Peak current is given in Fig. 5B. The Fig. 5C shows the linear plot of pH value vs oxidation peak potential and from this linear plot we can see that pH value has influence not only in peak current, but also in peak potential. The peak potential shifted to high positive potential as the value of pH increased from 3.0 to 9.0. This is an indication that protons are involved in the electrochemical oxidation process [45]. The linear relationship of pH and oxidation peak potential indicates pH dependency of electrocatalytic

activity of dopamine at flower shaped ZnO modified GCE. Further, the slope value is determined based on the linear plot given in Fig. 5C and is compared with the theoretical value. The slope value obtained from the linear plot is -58 mV/pH at 25°C and the theoretical value is -59 mV/pH. Therefore, the slope value calculated from the linear plot is almost equal to the theoretical value of -59 mV/pH calculated based on Nernst Equation [46]. This indicates that in the electrochemical oxidation of dopamine, same number of electrons and protons are involved [47, 48].

3.4 DPV and anti-interfering property evaluation of flower shaped ZnO modified GCE

The elimination of non-Faradaic current in DPV results in enhanced analytical signal and hence we have used DPV instead of CV for better analysis of sensitivity [49].
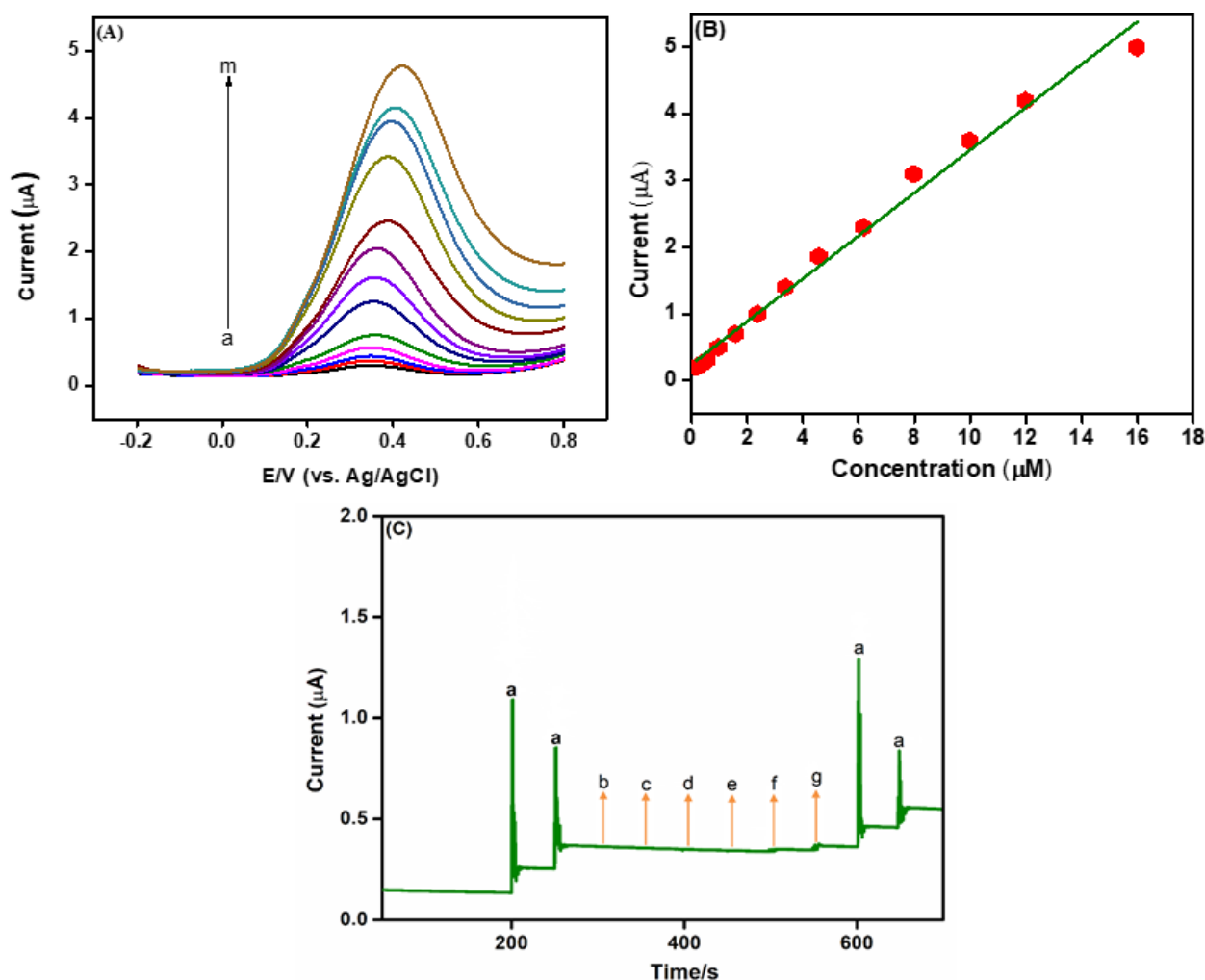
Figure 6. DPV curves of different concentrations of dopamine on flower shaped ZnO modified GCE in 0.05M PBS (pH 7.0) (A). Linear relationship between peak current and concentration of dopamine (B). Amperometric (*i-t*) responses at flower shaped ZnO modified RDGCE in the presence of successive additions of 10 μM dopamine and 50-fold excess solution of glucose, sucrose, gallic acid, uric acid, catechol and ascorbic acid (C).

Fig. 6A shows the DPV curves obtained for the detection of dopamine at flower shaped ZnO modified GCE. When we analyze the DPV curves, we can find that as the concentration of dopamine increases, their currents increased and the oxidation potential remained stable. As shown in Fig. 6B, the linear relationship between the dopamine concentration and current is in the linear range of 0.1-16 μM and the linear regression equation can be described as I (μA) = 0.3217x + 0.2436, R^2 = 0.9895 (0.1-16 μM). The limit of Detection (LOD) calculated from the linear plot is 0.04 μM and the sensitivity is 4.38 μAμM^{-1}cm^{-2}. Table 1 compares the linear range and LOD values of flower shaped ZnO modified GCE with other modified electrodes for the detection of dopamine. This comparative analysis point-out that flower shaped ZnO modified GCE is an apt electrode for the detection of dopamine.

Table 1. Comparative analysis of performance of flower shaped ZnO modified GCE with different electrodes for dopamine detection.

Modified Electrode	Detection Technique	Detection Limit (μM)	Linear range (μM)	Ref.
Graphene/AuNPs	DPV	1.86	5-1000	[50]
MWCNT/Fe$_3$O$_4$/2,3-Nc	DPV	1.77	2-25	[51]
GNF electrode	DPV	1.50	1.5-27.5	[52]
Au/RGO/GCE	DPV	1.40	6.8-41	[13]
Au/PE/PS/BBD	CV	0.80	5-100	[53]
AuNPs/PANI	Amperometry	0.80	3-115	[54]
Au Nanowire	Amperometry	0.40	0.4-250	[55]
GO	DPV	0.27	1-15	[56]
RGO-Pd-NPs	LSV	0.23	1-150	[57]
GO-MWCNT/MnO$_2$/AuNPs	Amperometry	0.17	0.5-2500	[58]
MgO/Gr/Ta	DPV	0.15	0.1-7	[59]
AuNPs/β-CD/GR	DPV	0.15	0.5-150	[60]
Ag-Pt/nanofiber	DPV	0.11	10-500	[61]
CNNS-GO	DPV	0.09	1–20	[62]
Fe3O4/r-GO/GC	DPV	0.08	0.4–3.5	[63]
AuNCs/AGR/MWCNT	SWV	0.08	1–210	[64]
GQDs–TiO2	CV	0.06	0.02-105	[65]
AuNPs/Trp-GR	DPV	0.05	0.5–411	[66]
Flower shaped ZnO	DPV	0.04	0.1 -16	This work

Selectivity is an important factor to be considered for an electrochemical sensor and thus studies to evaluate the selectivity is vital. We have evaluated the selectivity of the flower shaped ZnO modified RDGCE by using amperometric (*i-t*) technique. For this evaluation, we have selected 50-fold excess amount of regular interfacing biological compounds such as uric acid, ascorbic acid, gallic acid, catechol, sucrose and glucose. The concentration of dopamine considered for this study is 10 μM. From this study, it is found that the oxidation signal of dopamine is not affected by the presence of common interfacing biological compounds. The Fig. 6C shows the oxidation current signal of (a) dopamine in the presence of aforementioned common interfacing compounds including (b) glucose, (c) sucrose, (d) gallic acid, (e) uric acid, (f) catechol and (g) ascorbic acid. We observed exactly the same oxidation current signal for dopamine even in the presence of common interfacing compounds and this analysis is a proof for the good selectivity of flower shaped ZnO modified RDGCE.

3.5 Reproducibility, stability and repeatability of electrochemical sensor

For an electrochemical sensor, we have to consider various factors to evaluate its functionality. Hence, a thorough investigation is carried out to evaluate the stability, repeatability and reproducibility of the fabricated electrochemical sensor based on flower shaped ZnO nanoparticles. As the initial step, we have carried out the repeatability studies and for this, five successive measurements with relative standard deviation (RSD) of 2.36 % is taken using a single GCE modified by flower shaped ZnO nanoparticles. This study confirmed the excellent repeatability of the electrochemical sensor. In the next stage, to evaluate the storage stability, we have regularly monitored the anodic peak current of flower shaped ZnO modified GCE in the presence of 100 μM dopamine for 7 days. It is noted from the study that just a low percentage (6%) of anodic peak current response is reduced after 7 days when compared with its original peak current response. This study is a proof for the excellent storage stability of the flower shaped ZnO modified GCE. In order to evaluate the reproducibility of the electrochemical sensor, we have considered 5 independent flower shaped ZnO modified GCE with RSD of 3.14 % for the detection of dopamine and this study confirmed the excellent reproducibility of the flower shaped ZnO modified GCE.

3.6 Real sample analysis of dopamine

We have carried out dopamine detection in human serum and dopamine hydrochloride injection for the analysis of empirical feasibility of fabricated sensor in real samples. The dopamine injection sample is prepared by suitable dilution using 0.05M PBS (pH 7.0). For the real sample analysis to determine dopamine, we have followed the standard addition method. The resultant RSD and recovery of dopamine obtained from the real sample studies is described in Table 2. The recovery results of dopamine obtained from the experiment is in the range of 87.5% to 98.4% and the average recovery values for DA injection and human serum are 92.95% and 92.55% respectively. The proper recoveries obtained from real sample analysis confirms the feasibility of the proposed flower shaped ZnO modified electrode to be used in pharmaceutical formulations for the detection of dopamine.

Table 2. The determination of dopamine in real samples using flower shaped ZnO modified GCE.

Sample Name	Added (µM)	Found (µM)	Recovery (%)	RSD (%)
DA Injection	2	1.75	87.5	2.65
	5	4.92	98.4	3.08
Human Serum	2	1.81	90.5	2.89
	5	4.73	94.6	3.47

4. CONCLUSIONS

We have successfully developed a highly sensitive and selective electrochemical sensor based on flower shaped ZnO nanoparticles for the determination of dopamine. The flower shaped ZnO nanoparticles is synthesized using aqueous solution method without the addition of shape directing reagents. The crystal structure of flower-shaped ZnO nanoparticles is investigated by XRD and the analysis of surface morphology is carried out using SEM. This work proved that the electrocatalytic activity of the prepared flower shaped ZnO based GCE is excellent in the determination of dopamine and the sensor exhibited characteristics like good anti-interference potential, broad linear range, fast response, good reproducibility and repeatability. By analyzing all the results obtained from this work, we can conclude that flower shaped ZnO nanoparticles can be utilized as an apt electrode material for dopamine detection.

References

1.   H. Wang, S. Yao, Y. Liu, S. Wei, J. Su and G. Hu, *Biosens. Bioelectron.,* 87 (2017) 417-421.
2.   S. E. F. Kleijn, S. C. S. Lai, M. T. M. Koper and P. R. Unwin, *Angew. Chem. Int. Ed.,* 53 (2014) 3558-3586.
3.   X. Luo, A. Morrin, A. J. Killard and M. R. Smyth, *Electroanalysis,* 18 (2006) 319-326.
4.   W. Yang, K. R. Ratinac, S. P. Ringer, P. Thordarson, J. J. Gooding and F. Braet, *Angew. Chem. Int. Ed.,* 49 (2010) 2114-2138.
5.   A. Yu, Z. Liang, J. Cho and F. Caruso, *Nano Lett.,* 3 (2003) 1203-1207.
6.   J.-S. Jang, W.-T. Koo, S.-J. Choi and I.-D. Kim, *J. Am. Chem. Soc.,* 139 (2017) 11868-11876.
7.   P. K. Kannan, D. J. Late, H. Morgan and C. S. Rout, *Nanoscale,* 7 (2015) 13293-13312.
8.   Y. Li, W. Luo, N. Qin, J. Dong, J. Wei, W. Li, S. Feng, J. Chen, J. Xu, A. A. Elzatahry, M. H. Es-Saheb, Y. Deng and D. Zhao, *Angew. Chem. Int. Ed.,* 53 (2014) 9035-9040.
9.   I. Stassen, N. Burtch, A. Talin, P. Falcaro, M. Allendorf and R. Ameloot, *Chem. Soc. Rev.,* 46 (2017) 3185-3241.
10.   C.-H. Chen, S.-J. Chang, S.-P. Chang, M.-J. Li, I. C. Chen, T.-J. Hsueh and C.-L. Hsu, *Chem. Phys. Lett.,* 476 (2009) 69-72.

11.   K. Ghanbari and M. Moloudi, *Anal. Biochem.,* 512 (2016) 91-102.
12.   S.-H. Liao, H.-J. Jhuo, P.-N. Yeh, Y.-S. Cheng, Y.-L. Li, Y.-H. Lee, S. Sharma and S.-A. Chen, 4 (2014) 6813.
13.   C. Wang, J. Du, H. Wang, C. e. Zou, F. Jiang, P. Yang and Y. Du, *Sens. Actuators, B,* 204 (2014) 302-309.
14.   X. Zhu, I. Yuri, X. Gan, I. Suzuki and G. Li, *Biosens. Bioelectron.,* 22 (2007) 1600-1604.
15.   V. B. Kumar, K. Kumar, A. Gedanken and P. Paik, *J. Mater. Chem. B,* 2 (2014) 3956-3964.
16.   S. Mitra, S. B, P. Patra, S. Chandra, N. Debnath, S. Das, R. Banerjee, S. C. Kundu, P. Pramanik and A. Goswami, *J. Mater. Chem.,* 22 (2012) 24145-24154.
17.   A. Sachdev, I. Matai and P. Gopinath, *J. Mater. Chem. B,* 3 (2015) 1217-1229.
18.   S. Sardar, S. Chaudhuri, P. Kar, S. Sarkar, P. Lemmens and S. K. Pal, *Phys. Chem. Chem. Phys.,* 17 (2015) 166-177.
19.   G. Sberveglieri, C. Baratto, E. Comini, G. Faglia, M. Ferroni, A. Ponzoni and A. Vomiero, *Sens. Actuators, B,* 121 (2007) 208-213.
20.   C. S. Rout, S. Hari Krishna, S. R. C. Vivekchand, A. Govindaraj and C. N. R. Rao, *Chem. Phys. Lett.,* 418 (2006) 586-590.
21.   L.-J. Bie, X.-N. Yan, J. Yin, Y.-Q. Duan and Z.-H. Yuan, *Sens. Actuators, B,* 126 (2007) 604-608.
22.   C. Ge, Z. Bai, M. Hu, D. Zeng, S. Cai and C. Xie, *Mater. Lett.,* 62 (2008) 2307-2310.
23.   O. Lupan, L. Chow, S. Shishiyanu, E. Monaico, T. Shishiyanu, V. Şontea, B. Roldan Cuenya, A. Naitabdi, S. Park and A. Schulte, *Mater Res Bull,* 44 (2009) 63-69.
24.   T. Gao and T. H. Wang, *Appl. Phys. A,* 80 (2005) 1451-1454.
25.   Á. Németh, E. Horváth, Z. Lábadi, L. Fedák and I. Bársony, *Sens. Actuators, B,* 127 (2007) 157-160.
26.   G. She, X. Huang, L. Jin, X. Qi, L. Mu and W. Shi, *Small,* 10 (2014) 4685-4692.
27.   W. Sun, X. Wang, Y. Wang, X. Ju, L. Xu, G. Li and Z. Sun, *Electrochim. Acta*   87   (2013) 317-322.
28.   R. Zhang, G.-D. Jin, D. Chen and X.-Y. Hu, *Sens. Actuators, B,* 138 (2009) 174-181.
29.   X. Zheng, Y. Guo, J. Zheng, X. Zhou, Q. Li and R. Lin, *Sens. Actuators, B,* 213 (2015) 188-194.
30.   V. Hefco, K. Yamada, A. Hefco, L. Hritcu, A. Tiron and T. Nabeshima, *Eur. J. Pharmacol.,* 475 (2003) 55-60.
31.   F. Mora, G. Segovia, A. del Arco, M. de Blas and P. Garrido, *Brain Res.,* 1476 (2012) 71-85.
32.   D. L. Robinson, B. J. Venton, M. L. A. V. Heien and R. M. Wightman, *Clin. Chem.,* 49 (2003) 1763-1773.
33.   B. E. K. Swamy and B. J. Venton, *Analyst,* 132 (2007) 876-884.
34.   R. G. Holloway and K. M. Biglan, *Expert Opin Pharmacother,* 3 (2002) 197-210.
35.   J. W. Dalley and J. P. Roiser, *Neuroscience,* 215 (2012) 42-58.
36.   A. Galvan and T. Wichmann, *Clin. Neurophysiol.,* 119 (2008) 1459-1474.
37.   K. Jackowska and P. Krysinski, *Anal. Bioanal. Chem.,* 405 (2013) 3753-3771.
38.   J. M. Swanson and N. D. Volkow, *J. Child Psychol. Psychiatry,* 50 (2009) 180-193.
39.   F. Shi and C. Xue, *CrystEngComm* 14 (2012) 5407-5411.
40.   P. Bindu and S. Thomas, *J. Theor. Appl. Phys.,* 8 (2014) 123-134.
41.   S. Sakthinathan, S. Kubendhiran, S. M. Chen, K. Manibalan, M. Govindasamy, P. Tamizhdurai and S. T. Huang, *Electroanalysis,* 28 (2016) 2126-2135.
42.   S. A. Kumar and S. M. Chen, *Anal. Lett.,* 41 (2008) 141-158.
43.   Z. Zhao, W. Lei, X. Zhang, B. Wang and H. Jiang, *Sensors,* 10 (2010) 1216-1231.
44.   K. Mielech-Łukasiewicz, H. Puzanowska-Tarasiewicz and A. Panuszko, *Anal. Lett.,* 41 (2008) 789-805.
45.   K. Kurzątkowska, S. Sayin, M. Yilmaz, H. Radecka and J. Radecki, *Sensors,* 17 (2017) 1368.

46. M. Mazloum-Ardakani, H. Rajabi, H. Beitollahi, B. B. F. Mirjalili, A. Akbari and N. Taghavinia, *Int. J. Electrochem. Sci,* 5 (2010) 147-157.
47. F. Zhang, Y. Li, Y.-e. Gu, Z. Wang and C. Wang, *Microchim. Acta,* 173 (2011) 103-109.
48. M. Lv, T. Mei, C. a. Zhang and X. Wang, *RSC Adv.,* 4 (2014) 9261-9270.
49. A. Chen and B. Shah, *Anal. Methods,* 5 (2013) 2158-2173.
50. J. Li, J. Yang, Z. Yang, Y. Li, S. Yu, Q. Xu and X. Hu, *Anal. Methods,* 4 (2012) 1725-1728.
51. N. G. Mphuthi, A. S. Adekunle, O. E. Fayemi, L. O. Olasunkanmi and E. E. Ebenso, *Sci. Rep.,* 7 (2017) 43181.
52. W. Humers and R. Offeman, *J. Am. Chem. Soc.,* 80 (1958) 1339.
53. M. Wei, L. G. Sun, Z. Y. Xie, J. F. Zhii, A. Fujishima, Y. Einaga, D. G. Fu, X. M. Wang and Z. Z. Gu, *Adv. Funct. Mater.,* 18 (2008) 1414-1421.
54. A.-J. Wang, J.-J. Feng, Y.-F. Li, J.-L. Xi and W.-J. Dong, *Mikrochim Acta,* 171 (2010) 431-436.
55. P. Tyagi, D. Postetter, D. Saragnese, C. Randall, M. Mirski and D. Gracias, *Anal. Chem.,* 81 (2009) 9979-9984.
56. F. Gao, X. Cai, X. Wang, C. Gao, S. Liu, F. Gao and Q. Wang, *Sens. Actuators, B,* 186 (2013) 380-387.
57. S. Palanisamy, S. Ku and S.-M. Chen, *Mikrochim Acta,* 180 (2013) 1037-1042.
58. D. Rao, X. Zhang, Q. Sheng and J. Zheng, *Mikrochim Acta,* 183 (2016) 2597-2604.
59. L. Zhao, H. Li, S. Gao, M. Li, S. Xu, C. Li, W. Guo, C. Qu and B. Yang, *Electrochim. Acta,* 168 (2015) 191-198.
60. X. Tian, C. Cheng, H. Yuan, J. Du, D. Xiao, S. Xie and M. M. Choi, *Talanta,* 93 (2012) 79-85.
61. Q. Lian, A. Luo, Z. An, Z. Li, Y. Guo, D. Zhang, Z. Xue, X. Zhou and X. Lu, *Appl. Surf. Sci.,* 349 (2015) 184-189.
62. H. Zhang, Q. Huang, Y. Huang, F. Li, W. Zhang, C. Wei, J. Chen, P. Dai, L. Huang, Z. Huang, L. Kang, S. Hu and A. Hao, *Electrochim. Acta,* 142 (2014) 125-131.
63. H. Teymourian, A. Salimi and S. Khezrian, *Biosens. Bioelectron.,* 49 (2013) 1-8.
64. A. A. Abdelwahab and Y.-B. Shim, *Sens. Actuators, B,* 221 (2015) 659-665.
65. Y. Yan, Q. Liu, X. Du, J. Qian, H. Mao and K. Wang, *Anal. Chim. Acta,* 853 (2015) 258-264.
66. Y. Huang, Y.-E. Miao, S. Ji, W. W. Tjiu and T. Liu, *ACS Appl. Mater. Interfaces,* 6 (2014) 12449-12456.